

Power Management Optimization for Off-Design Performance Assessment of Ducted Electric Fan with Boundary Layer Ingestion

Joseph Brucculeri*, Luis Salas Nunez†, Jonathan Gladin‡, and Dimitri N. Mavris§
Georgia Institute of Technology, Atlanta, Georgia, 30332

This work consists on the examination of the system level benefits of a partially turbo-electric propulsion architecture with Boundary Layer Ingestion (BLI) in a 150-pax class size commercial aircraft. This propulsion system consists of an electric ducted fan that ingests the boundary layer from the aft-end of the fuselage. The power for this aft-fan is extracted from two underwing turbofan engines. The BLI effects are quantified in CFD using the power balance method, which are then integrated using surrogate models into an aircraft sizing and mission analysis environment to obtain mission performance metrics. With the overarching goal of minimizing fuel consumption, an approach to optimize the motor power during off-design analysis is presented. The effect that different power management strategies have on system performance are also analyzed. The results showed that such novel propulsion architecture not only presents benefits with respect to a conventional system, but also that the application of an optimized power schedule offers additional fuel burn reductions.

Nomenclature

A_N	=	nozzle area
C_D	=	drag coefficient
$\Delta\Phi_{wake}$	=	change in wake viscous dissipation rate
$D_{spillage}$	=	spillage drag
D_{WM}	=	wind-milling drag
e_{Ram}	=	inlet pressure recovery
\dot{E}	=	mechanical energy outflow rate
F_{BLI}	=	boundary layer ingestion thrust benefit
FPR	=	fan pressure ratio
F_X	=	net streamwise force
F_{net}	=	gross net thrust
LPC_{SMW}	=	low-pressure compressor stall margin
\dot{m}	=	mass flow rate
M_∞	=	free-stream Mach number
$N_{C_{max}}$	=	aft-fan max speed
PC	=	power code
p_s	=	static pressure
P_K	=	net propulsor mechanical energy flow rate
Φ_{surf}	=	airframe viscous dissipation rate
$TSFC$	=	thrust specific fuel consumption
T_s	=	static temperature
V_∞	=	free-stream flow velocity
V_N	=	nozzle flow velocity

*Graduate Research Associate, Aerospace Systems Design Laboratory, AIAA Student Member

†Graduate Research Associate, Aerospace Systems Design Laboratory, AIAA Student Member

‡Research Engineer II, Aerospace Systems Design Laboratory, AIAA Member

§S.P. Langley Distinguished Regents' Professor and Director of ASDL, School of Aerospace Engineering, AIAA Fellow

I. Introduction

BOUNDARY Layer Ingestion (BLI) and wake filling have been the focus of extensive research in the past decades. Even though it has not been successfully incorporated into an aircraft yet, it is an idea that has gained significant attention in the past years. Multiple studies have pointed out similar trends in how BLI reduces power consumption and improves propulsive efficiency. This led to BLI being recognized as a possible enabler for high efficient commercial aircraft concepts [1]. Various concepts featuring BLI have been formulated, such as Hybrid-Wing-Body (HWB) configurations, the "double-bubble" D8 concept, and the STARC-ABL.

The subject of study of this paper is a propulsion architecture like the STARC-ABL. This is a vehicle concept with dimensions similar to a notional tube-and-wing 150-pax aircraft that employs a partial-turboelectric propulsion architecture, where power is extracted from underwing turbofan engines to power a ducted electric fan in the aft of the fuselage (see Fig. 1). This concept, originally proposed by Welstead and Felder, has been subject of continuous research and design refinements. Whereas initial estimates concluded that this architecture could reduce economic mission block fuel by 15.2% [2], the latest published result only shows a 2.7% benefit [3].

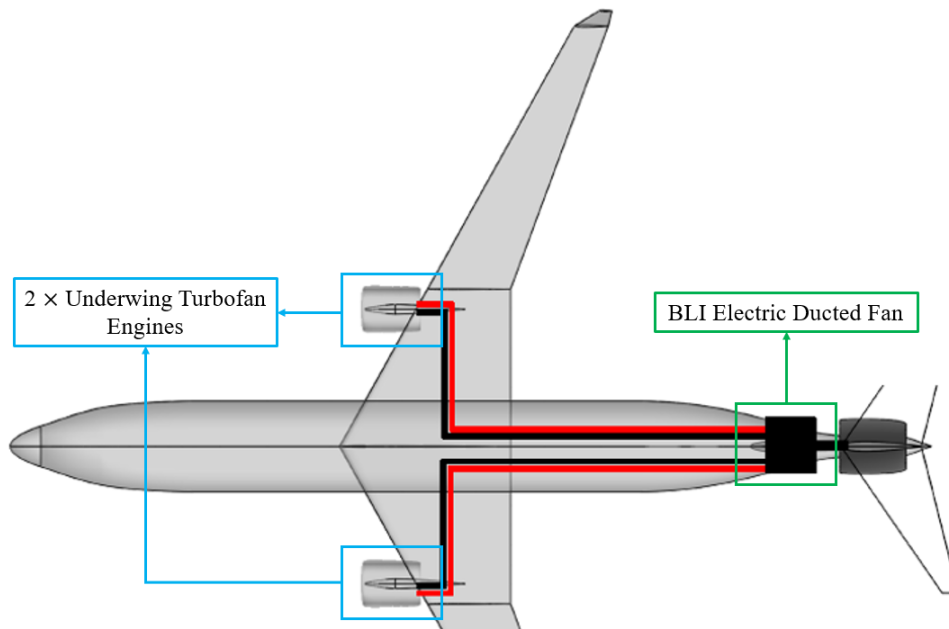


Fig. 1. STARC-ABL Concept [2]

There is, however, some level of uncertainty in regards to the benefits that this propulsion architecture can provide to the overall system performance. Besides the previously mentioned differences between the initial and the revised fuel burn benefits, recent work by Hall et al. [4], concluded that this turboelectric architecture does not represent a significant improvement with respect to a "more conventional" aircraft system in the far-term time frame. Additional work has been done to attempt to optimize the benefits from this BLI configuration, by either minimizing flow distortion using aerodynamic shape optimization [5], or the minimization of shaft power with respect to nacelle design, engine cycle parameters, and energy transmission efficiency [6].

This work examines the off-design performance of this type of propulsive architecture with the goal of determining optimal level of electric motor power throughout various mission segments. In order to do so, the "power balance" method is applied to quantify the BLI impacts in propulsor performance, which were then integrated into an aircraft design and mission analysis environment. This required the identification of proper operability constraints on the aft-fan, and the implementation of a single variable optimization algorithm to minimize fuel burn through the aircraft's flight envelope. This analyzed reveals trends between thrust specific fuel consumption (*TSFC*), total thrust, and the aforementioned power management strategy.

A. Boundary Layer Ingestion

The concept of boundary layer ingestion, or the more general case of wake filling, has been subject of study for a long time, with some of the first studies published in the mid-1940s [7]. To illustrate the concept of BLI and its benefits, consider the schematic presented in Fig. 2. It shows three different representations of a fuselage and its wake. The top is a fuselage alone with no BLI system, where it can be seen that the presence of the fuselage in a flow creates a wake behind it (represented by a defect in the flow’s kinetic energy). The second shows a propulsor mounted on top of the aft-end of the fuselage, ingesting boundary layer flow (such as in the D-8 concept). Finally, the third image shows another BLI configuration, where the nacelle encircles the aft-end of the fuselage, ingesting boundary layer from both the top and bottom surfaces of the fuselage (like the STARC-ABL).

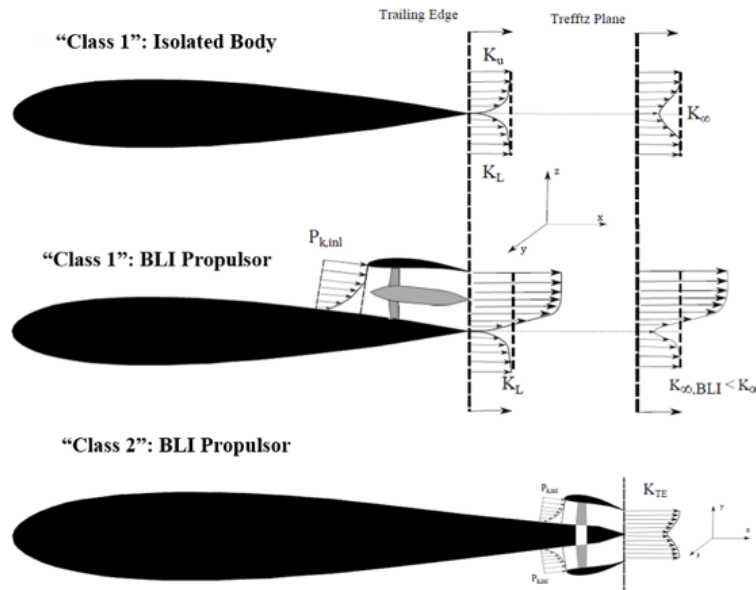


Fig. 2. Schematic of Boundary Layer Ingestion Configurations [8]

Figure 2 shows how adding this BLI propulsor in the aft-end re-energizes the wake, reducing energy losses. If the flow behind the fuselage was restored back to freestream velocity, there would not be a momentum deficit. There is also a reduction in power dissipation and jet mixing losses, which are basically sources of wasted kinetic energy [9]. Such case is known as “ideal wake filling”, and represents the maximum theoretical benefit from this configuration. Other possible benefits come from the fact that boundary layer flow is at a lower speed with respect to the free stream. Therefore, for the same mass flow rate, a BLI engine requires less power to impart the required momentum change to generate thrust, increasing propulsive efficiency. Finally, this slower boundary layer flow produces less ram drag, which is the momentum deficit produced as the flow is slowed down and ingested by the inlet.

However, ingesting boundary layer flow proposes many challenges that still need to be addressed. Mainly, there are several performance penalties associated with the loss in total pressure (which represents lower availability to do work and produce thrust), in addition to the fan efficiency losses and additional stress in the blades. Furthermore, the placement of the engine in the aft-end requires a careful integration with the airframe, since flow separation can become an issue at many flight conditions [8]. This engine also needs to be integrated with the overall power generation and distribution architecture, increasing the complexity of the design.

B. BLI Analysis Methods

In general, multiple studies have concluded that BLI can produce both propulsive and aerodynamic benefits. These benefits are often expressed in terms of reductions in fuel consumption, increased propulsive efficiency, and greater L/D, as shown by Blumenthal [7]. Smith [10] performed the theoretical development which many of the modern studies have used as reference. His main contribution was the development of the Power Saving Coefficient (PSC), a figure of merit that compares the power used by a BLI system in comparison to an equivalent non-BLI one. Smith also started the discussion on the definition of propulsive efficiency for these cases, since the well-known Froude efficiency definition

was no longer appropriate to represent the physics of the problem. Finally, Smith came up with the first formal analysis methodology to perform BLI studies by linking propulsor performance with respect to boundary layer parameters.

Recent research in BLI has shown two main trends: in one hand, there is the effort to quantify the BLI benefits using a conventional momentum-balance approach, which leads to traditional thrust and drag terms. On the other hand, there is an argument about how conventional "thrust-drag" bookkeeping methods are not appropriate for BLI concepts, and hence it is necessary to use a "Power-Balance approach" to quantify these effects [9]. In addition, it is necessary to recognize the multidisciplinary nature of the BLI impacts. Hendricks [11], summarizes the work done by different authors in this matter, and recommends the use of strongly coupled approaches that integrate both aerodynamic and propulsive analysis methods.

II. Modeling Approach and Implementation

This work builds on top of the observations made by different authors and the available literature on the subject. Here, the BLI effects are quantified using a coupled aerodynamic-propulsive approach between CFD simulations (using STAR-CCM+) and a 1-D propulsion cycle analysis tool (NPSS). These effects are later integrated into an optimization routine, as described in the next section. All of these analysis routines are wrapped under the Environmental Design Space (EDS) tool. This section is dedicated to provide details of the entire implementation process.

A. NPSS Propulsion Model

The Aerospace Systems Design Lab (ASDL) has conducted research on various hybrid and turbo-electric concepts [12]. These studies led to the development of NPSS elements capable of modeling generic electric components that did not exist in the standard library of elements [13]. These include conventional motor and generators, power conditioning components such as inverters and rectifiers, and power distribution components like cables and buses. The motor and generator elements are modeled based on the physics for a switch reluctance motor and include models for windage, copper, and iron losses. They have the flexibility to determine the component efficiency when shifting from the design points to other operating conditions. The rest of the components are assumed to have a constant efficiency and are used to model the power distribution system and book keep the electrical state in between the components.

Modeling the electrical components as separate elements allows calculating their thermal loads independently. This calculation is made based off their power losses as a function of their efficiency. In a partial-turboelectric architecture such as the one being studied here it is necessary to include additional calculations for the thermal management systems, as they are additional power draws from the main source of power. Power cables, on the other hand, are assumed to have enough insulation and surface to not require any thermal management system.

These electric elements are assembled with a geared fan model, which represents the under-wing turbofan engines. From here, power is extracted from the low-pressure shaft to power a generator. This energy is then transmitted by a series of elements to the electric motor that drives the BLI fan. This propulsion architecture is represented in Figure 3.

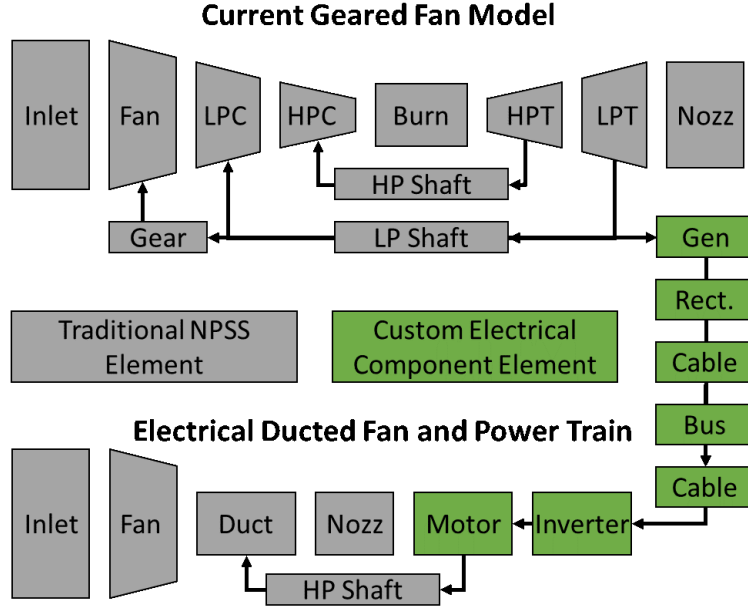


Fig. 3. Partially-turboelectric Propulsion Architecture

The aft-fan propulsor is modeled in NPSS using a custom inlet element with a typical compressor, duct, and nozzle elements. The custom inlet element was modified with custom sockets to handle calculations for accounting for the BLI effects (i.e. the surrogate models) and additional drag terms such as spillage and wind-milling (at low power). Spillage is determined as a function of the free stream Mach number ratio between the inlet's capture area and the free stream's physical flow area as defined in [14]. Wind-milling, on the other hand, is determined using a method by Torenbeek [15], which calculates this additional drag using Eq. 1.

$$\Delta(C_{DS})_{WM} = \frac{2}{1 + 0.16M_\infty^2} A_N \frac{V_N}{V_\infty} \left(1 - \frac{V_N}{V_\infty}\right) \quad (1)$$

B. Quantifying the BLI Benefits

The estimation of the BLI benefits and the conceptual design stage proposes many modeling challenges. Gray, for instance, demonstrated how it is necessary to employ coupled aero-propulsive analyses in order to properly capture its impacts. This was revealed by examining trends between Fan Pressure Ratio (FPR) and net stream-wise force (F_X) [16]. On the other hand, Hall highlights how in a BLI configuration, the flow around the airframe is affected by the pressure fields generated by the propulsor [9]. Therefore, the use of conventional momentum analysis techniques becomes inappropriate to assess thrust and drag.

A more recent paper by the same author compares the momentum-based approach against the power-balance approach and presents a method to use CFD for the quantification of the BLI impacts [17]. Similarly, Pokhrel [18] demonstrated how to quantify the BLI effects in CFD using the power balance framework, and then integrate the results from these simulations in a propulsion analysis code by using surrogate models. This method was used to illustrate trends of BLI effects on a concept similar to the one being examined here, and provided more evidence on the need to employ coupled aero-propulsive models.

The present work uses a similar approach as Pokhrel, where the BLI effects are quantified in CFD by calculating the following quantities:

$$P_{K_{inlet}} = \iint -[(p - p_\infty)\hat{n} + \frac{1}{2}\rho(V^2 - V_\infty^2)]V \cdot \hat{n}dS_{inlet} \quad (2)$$

$$\Delta\Phi_{wake} = \frac{P_{K_{inlet}}}{\Phi_{surf}} \Phi'_{wake} = \dot{E}_{out} \quad (3)$$

$$eRam = \frac{P_{t_{inlet}}}{P_{t_{\infty}}} \quad (4)$$

The propulsion model shown in Fig. 3 was used to obtain a set of boundary conditions to be used in CFD. In this model, the solver was setup to vary the aft-fan mass flow to hit a target shaft power. Then, the operating conditions as well as input shaft power were varied to represent the operation of the aft-fan at different points in the flight envelope. The boundary conditions consisted of mass flow (\dot{m}), flow properties at the fan-face (p_s and T_s) and fan-exit (p_t and T_t) for a given Mach and altitude combination. The goal was to represent the operation of the aft-fan at different points in the flight envelope and under different power settings. This process was repeated for three different blade heights, with the purpose of enabling the parametric variation of the propulsor geometry. This data was then used to setup powered CFD simulations in STAR-CCM+.

The geometry used was a 2-D axisymmetric model, consisting of a fuselage with dimensions similar to the STARC-ABL, whose aft part was modified to mount a ducted fan propulsor. In this model, the fan-face was modeled as a *pressure outlet*, and the fan-exit was set as a *stagnation inlet*. The responses tracked consisted of inflow mechanical flow rate ($P_{K_{inlet}}$), inlet total pressure recovery ($eRam$), and changes in wake dissipation ($\Delta\Phi_{wake}$). Convergence was achieved by varying the fan-face static pressure boundary condition until the CFD converged to the same mass flow as predicted by NPSS.

The outputs from the CFD simulations were then post-processed using the JMP statistical software. The power terms were normalized with respect to free stream flow conditions. Surrogate models were created to represent the responses of interest as a function of Mach, altitude, blade height, and corrected mass flow. These surrogate models consisted of response surface equations which were coded into the NPSS elements. This allowed NPSS to rapidly calculate $P_{K_{inlet}}$ and $\Delta\Phi_{wake}$ (for each operating condition) which were then used to estimate an equivalent BLI benefit as follows:

$$F_{BLI} = \frac{P_{K_{inlet}} + \Delta\Phi_{wake}}{V_{\infty}} \quad (5)$$

This BLI benefit is then added to the gross thrust predicted by the cycle analysis. Here, $P_{K_{inlet}}$ represents an equivalent ram drag reduction due to the propulsor ingesting boundary layer flow, whereas $\Delta\Phi_{wake}$ is used to quantify the reduction in the wake dissipation losses due to the jet flow filling part of this wake. It is also worth noting that the surrogate for $eRam$ accounts for the lower total pressure ingested by the propulsor, which decreases the capability of the fan to produce thrust. The BLI benefits, however, are greater than this *penalty*. Here, the term "*penalty*" has to be used with caution, as both $P_{K_{inlet}}$ and $eRam$ are connected. This entire process is represented in Fig. 4, which shows the data flow in this coupled aero-propulsive approach.

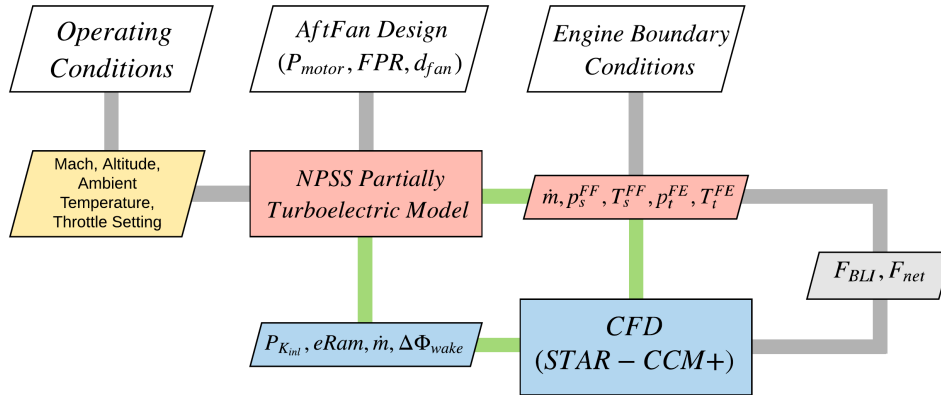


Fig. 4. Coupled Aero-propulsive Analysis Schematic

C. System-level Analysis

The NPSS model shown in Fig. 3 is integrated within ASDL's Environmental Design Space (EDS) tool [19]. This tool allows the design and evaluation of multiple aircraft architectures, and has been extensively developed and tested

throughout the years [20]. This tool contains multiple analysis routines and codes, such as FLOPS, WATE, CMPGEN, and many more, as seen in Fig. 5. It also has the capability to perform multi-design point (MDP) on-design cycle analysis, which ensures that the resulting architecture is capable of meeting design requirements and constraints at many points in the flight envelope [21].

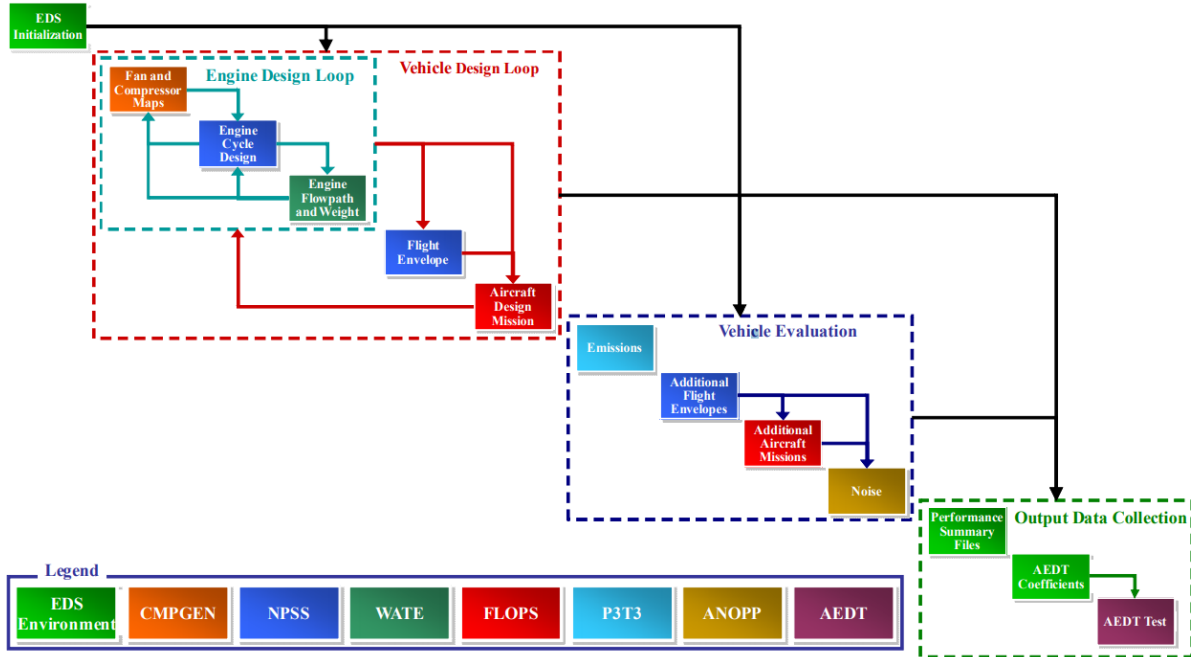


Fig. 5. EDS Assembly Schematic

In this framework, the vehicle is modelled by a mission, air-frame, and engine assembly. The mission assembly allows the definition of a custom mission profile containing segments such as taxi, takeoff, climb, cruise, etc. This assembly provides the vehicle the current ambient operating conditions, which are then passed to the air-frame assembly to determine the vehicle’s required thrust. Finally, the engine assembly contains the propulsion system’s cycle model. The operation design points for the engine are cruise, top of climb, take off, installed and uninstalled sea-level static.

It is important to note that this work required the inclusion of electric elements which were not previously available in EDS, but rather were part of GT-HEAT, another ASDL tool created specifically for the analysis of electric propulsion architectures [12]. Modeling such a unique propulsion system brings additional challenges and complications compared to traditional engine cycle balancing. The electrical components and BLI propulsor provide additional design parameters and constraints that need to be handled by the NPSS solver during the MDP analysis and off-design simulations.

The total propulsion system weight and flowpath analysis is calculated and bookkept using WATE++. This analysis also included the calculation of the additional turbo-electric elements, which followed the assumptions that NASA has made for their far-term vehicle concepts [3], presented in Table 1. With the aft-fan motor power constrained to a max rated power, the design powers for the rest of the components are determined during the MDP analysis. Thermal loads are calculated based on cooling requirements, which are calculated for each element and then summed up. Then, the specific power is used to find the weight of the system. Finally, cable weights are determined using the method from Campbell’s dissertation [22].

Table 1. Electrical Component Assumptions

Component	Efficiency (%)	Specific Power (hp/lb)
Generator	96.0	8.0
Motor	96.0	8.0
Invertor	98.0	11.6
Rectifier	98.0	11.6
Thermal Management	-	0.42

D. Off-Design Mission Analysis and Power Management

Going back to the partial-turboelectric propulsion architecture displayed in Fig. 1, the initial design considered a constant power input to the motor that drives the BLI fan throughout the mission [2]. This aft-fan was also sized to provide 1/3 of the thrust at cruise condition. The main research objective that motivated this work was to explore different types of power management schedules. The hypothesis is that it is possible to find optimal values of off-design electric motor power that improves the overall mission fuel burn. Figure 6 shows three different power management examples throughout the mission.

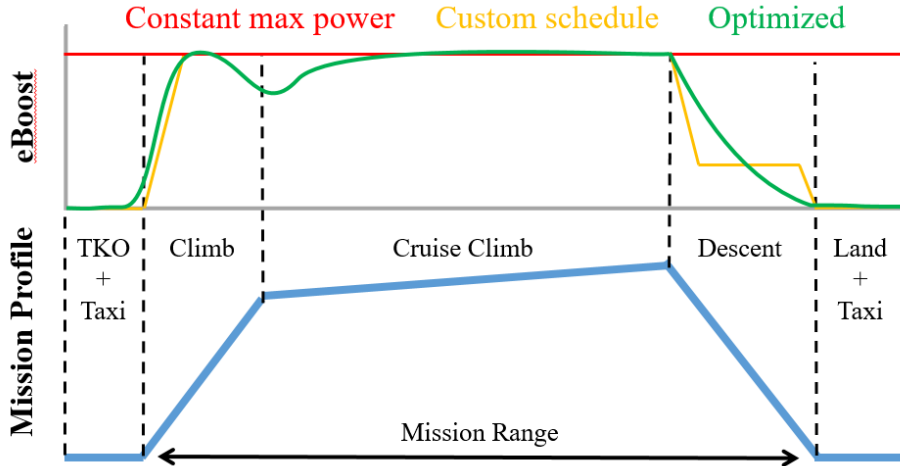


Fig. 6. Motor Power Management Options

In the EDS environment, the flight envelope is evaluated by running the NPSS model in a series of off-design cases. The cases shift through flight conditions in increments of Mach No. and altitudes in order to generate an engine deck that can be used by FLOPS. This deck contains data such as engine thrust and fuel flow for the entire flight envelope at the max power/thrust setting, as well as part power settings. To find the maximum thrust, the NPSS model is set up to vary fuel flow (regularly represented by the fuel-to-air ratio) to hit a target maximum fan speed (set by its stall margin). For the part-thrust, however, a target percentage thrust is defined using a Power Code (*PC*). This PC ranges from 50 (max thrust) to 21 (5% max thrust), and the solver is instead setup to vary fuel flow in order to match the thrust target.

For a traditional gas turbine engine, this is a straight forward process. For the partially turbo-electric system, on the other hand, there are two sources of thrust. This opens up different possibilities for power management and thrust splits. One can set max thrust by setting the aft-fan motor to its max rated power. Part-power settings can be simulated by throttling down either the turbofans or the aft-fan. However, what is the power management strategy that yields the lowest mission fuel consumption? In this work, this is treated as an optimization problem, which is formally set up as shown in Table 2:

Table 2. Power Management Optimization Problem Setup

	Variable	Description
minimize	$TSFC$	Thrust Specific Fuel Consumption
with respect to	P_{motor}	Aft-fan Motor Power
subject to	P_{max}	Max. Rated Power
	$Turbofan\ Idle$	Operating limit
	$N_{C_{max}}$	Aft-fan Max. Speed
	LPC_{SMW}	Compressor Stall Margin

Here the objective function is to minimize $TSFC$ for each mission segment by varying the electric motor power. This problem was approached by using a one dimensional Golden search algorithm [23], which is setup as an NPSS optimizer class. This is a generic class, written by Konstantinos Milios from ASDL, that can be added to any NPSS assembly to optimize single objective variables. For the algorithm to be successfully implemented in NPSS, it was necessary to establish reasonable bounds (max/min) of motor power to ensure the model converges during each iteration. These are setup as follows:

- **Maximum Motor Power:** at first glance, one might think that max power is simply the max motor design power. However, motor power directly sets the amount of thrust produced by the aft-fan. Hence, it is necessary to constraint the amount of thrust that the aft-fan produces in order to avoid going over the thrust target (as set by PC). Additionally, there is a minimum bound imposed on the turbofan net thrust (*turbofan idle*). Without this constraint, the previous set up can converge to a point where the aft-fan is running at max power but is solely producing more thrust than the target value. To compensate, the turbofan "produces" more drag than thrust, which is not a realistic representation of the physics of the system.
- **Minimum Motor Power:** just as the last setup, the solver is set to achieve a target F_{net} . In this case, the aft-fan mass flow drives it to produce zero net thrust. During the MDP analysis, the turbofans are sized with the aid of the aft-fan propulsor to meet a thrust requirement. In the case when the aft-fan does not produce any force, the turbofans has to produce the entire force to meet the requirement. In some cases, this puts a high demand on the turbofan, which might lead to compressor stall issues. To prevent this, a minimum low-pressure compressor stall margin (LPC_{SMW}) constraint was added to the solver.

As for the optimization function itself, the optimizer is run while producing the throttle hooks. It first finds the min/max bounds, then executes the 1-D line search to find the optimal motor power for each condition (Mach, altitude, and PC), and saves the values to the engine deck file. Furthermore, an alternative baseline schedule was produced to compare the optimizer results. In this baseline, the aft-fan is run at its max motor power value ($PC = 50$), whereas the turbofan thrust is adjusted to meet the remainder of the net thrust requirement. The ratio of aft-fan thrust to underwing engines thrust is calculated and then kept constant for the other part thrust runs. This is referred to as a constant thrust split case.

III. Results

The previously described partial-turboelectric propulsion architecture (Fig. 3) and sizing environment (Fig. 5) were used to size the BLI electric aft-fan and then examine different power management schedules with the objective of minimizing fuel consumption. This section describes the resulting engine cycle designs, the motor power operational space, and the performance of four different power management strategies: 1) optimal motor power, 2) maximum motor power, 3) minimum motor power, and 4) constant thrust split.

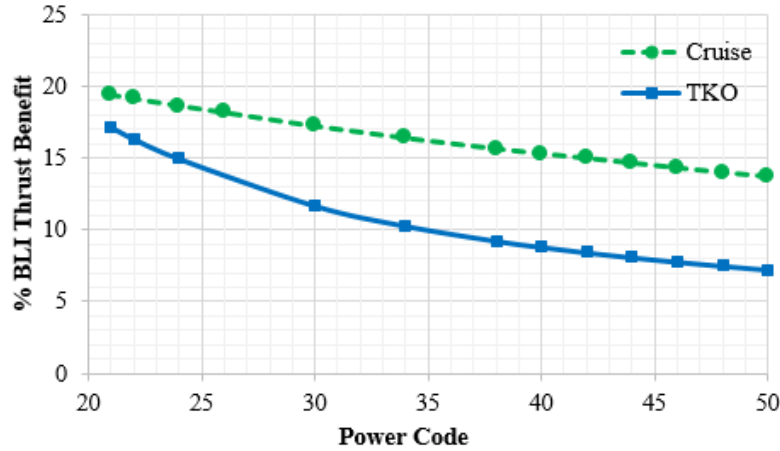
A. BLI Propulsor Design

In this framework, a multi-design point (MDP) analysis was performed for the entire partial-turboelectric propulsion architecture. The performance of this system was examined at critical points such as the Aerodynamic Design Point (ADP), Top-of-Climb (TOC), and Take-off (TKO). To start, Table 3 summarizes the aft-fan design and performance at the ADP.

Table 3. Aft-Fan Propulsor Design at ADP

Variable	Value
Altitude (<i>ft</i>)	35000
Mach No.	0.785
FPR	1.25
Mass Flow (<i>lbm/s</i>)	345.85
Motor Power (<i>hp</i>)	3500.0
Thrust (<i>lbf</i>)	2310.0
Thrust/HP ratio (<i>lbf/hp</i>)	0.660
Fan Diameter (<i>in</i>)	74.0

The resultant BLI propulsor was compared against an equivalent propulsor that ingests free-stream air in order to get an idea of the BLI benefits. This was done by running the model at the same operating conditions but without any F_{BLI} benefit (Eq. 5) and with an inlet pressure recovery set to a constant 0.995. This was done at multiple power codes and for both take-off (TKO) and ADP. The results are shown in Figure 7.

**Fig. 7. Aft-Fan BLI Thrust Benefits**

As shown in Fig. 7, this BLI electric propulsor offers superior performance than a conventional propulsor in terms of thrust generation. This benefit is significantly greater at cruise conditions than take-off, which provides a glimpse into the way the BLI fan should be used. A breakdown of the BLI cruise performance shows that the benefits come mostly from the ram drag reductions and, in a smaller percentage, the reduction in wake dissipation losses. Now, the fuel consumption performance of the entire partial-turboelectric propulsion architecture is compared against an equivalent Far Term geared fan underwing cycle for both TOC and ADP. The results, shown in Table 4, shows a reduction of roughly 3% in $TSFC$ at the two design points.

Table 4. Engine Cycle TSFC Performance Comparison

Mission Point	Partial-Turboelectric	Far Term Geared Fan	% Difference
ADP	0.4844	0.4990	-2.93
TOC	0.4867	0.5010	-2.85

B. Motor Power Operational Space

With the previous point-design performance results, now it was desired to employ the optimization algorithm previously described to explore the upper and lower bounds of motor power at different phases of the mission flight envelope and for different power codes. In addition, an optimal level of power that minimizes TSFC was found within those bounds. This analysis is summarized in Figure 8 for both take-off and ADP conditions. The resulting powers were normalized with respect to the motor max rated power of 3,500 hp.

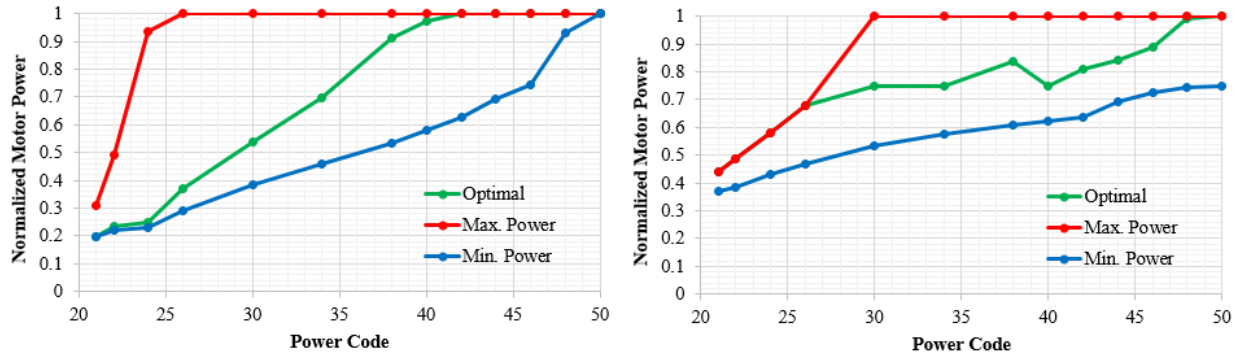


Fig. 8. TKO (Left) and ADP (Right) Motor Operational Space

Observation of the results shows that the two operational spaces are unique. The slopes for the upper and lower bounds vary at different part powers and no pattern can be observed between the flight conditions. Starting from the max power condition ($PC = 50$), both analyses show that optimal power is at this max design power. However, once the engine is throttled down, the optimal motor power line behaves differently between the two conditions. At TKO, optimal motor power is the max rated power until $PC < 40$ (approximately 66% of max thrust). This is due to the propulsor's spillage drag, which increases with Mach No. and mass flow rate [24]. For lower PCs, optimal power decreases until hitting the lower allowable power bound.

On the other hand, at the ADP, optimal motor power is shown to be closer to the max allowable power at all throttle settings. This is an indication of how the BLI aft-fan propulsor is more efficient at producing thrust at cruise conditions, as it was shown in Fig. 7.

C. Power Management Schemes

After examining the engine cycle performance at some critical design points and identifying the behavior of the motor power operational space, it is now desired to determine the impact of using different power management alternatives throughout the mission. This was done by using the NPSS propulsion model to generate engine decks, which were then parsed into an aircraft sizing and mission analysis routine. The engine deck generation process starts by simulating the performance of the system at max power and low altitudes. Then, the model is throttled down (from $PC = 50$ to $PC = 21$). This process is repeated for a set of altitudes and Mach numbers that cover the entire aircraft envelope. Now, when simulating the model at lower thrust settings, four different power management schemes were used:

- 1) **Optimal motor power:** the optimization algorithm described in the earlier section is used.
- 2) **Maximum motor power:** the model is simulated to operate at the highest motor power possible using the set-up described earlier.
- 3) **Minimum motor power:** just as above, but with the model operating at the lowest motor power possible.
- 4) **Constant thrust split:** the ratio between the thrust provided by the turbofans and aft-fan at max power is kept constant as it is throttled down for a given altitude and Mach number.

Using the engine decks generated by each one of these power management options, it was possible to find the *TSFC* reduction percentages with respect to the baseline cycle at any flight condition and throttle setting. Figure 9 shows these reductions for both takeoff and cruise. Note that in this figure a positive quantity implies a reduction in *TSFC*.

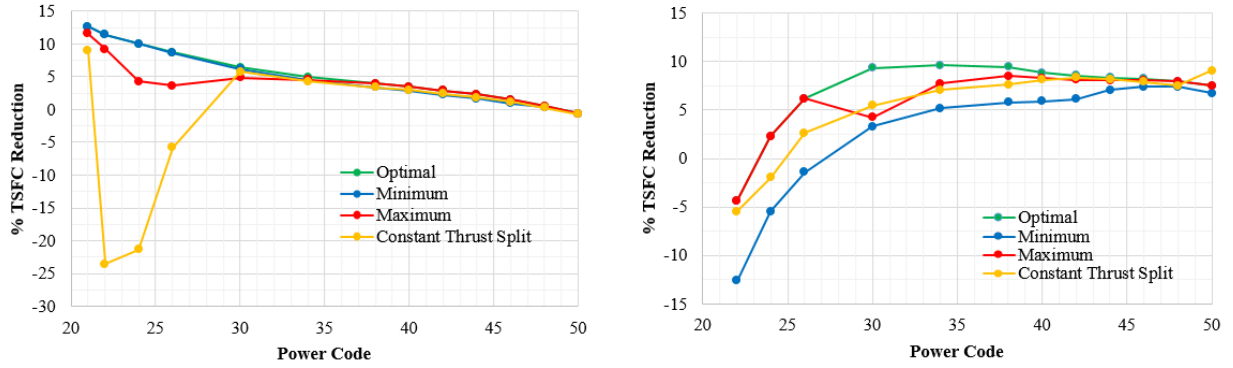


Fig. 9. TKO (Left) and Cruise (Right) % TSFC Reduction with Power Management Option

At first glance it is evident that the benefits offered by this propulsion architecture are lower at TKO than at cruise, a result that has been reported before. In the same way, the TKO data shows that there is virtually no difference in regards to the power management strategy used for $PC > 35$, which indicates that the motor power for all schemes is the same and there is no room to produce benefits from the optimizer. At low PCs, the optimal power is closer to the minimum allowable power, consistent with what was shown in Fig. 8. When it comes to the cruise data, running at optimal motor power results in the highest reduction in $TSFC$, as expected. It is noted that, at cruise, the maximum power always results in the closest $TSFC$ reduction to optimal power. Minimum power, on the other hand, results in half of the % $TSFC$ reduction.

The fourth power management scheme, constant thrust split, is an intuitive way to throttle down both turbofan and propulsor equally. The previous analysis shows that this approach results in average performance in terms of $TSFC$ reduction. It is not as close to the optimal power's $TSFC$ reduction as the other power management schemes but also does not often results in the lowest reduction. It is also clear how this strategy could be detrimental to fuel consumption at low PCs. This is due to the motor operating at a power below the minimum power line, and highlights the importance of properly identifying the upper and lower bounds for the operation of the aft-fan. The minimum allowable power is constrained by turbofan idle limits and aft-fan wind milling effects. These constraints were not active in the NPSS model for this power management strategy.

The ratio between turbofan and propulsor were also examined and are shown in Fig. 10 for both ADP and TOC. From max power to 40 PC (66% max thrust), operating at optimal motor power results in the thrust ratio not varying more than 5%. As the throttle setting lowers, in order to perform optimally, the aft-fan should not be throttled down at the same rate as the turbofan. For low PCs at cruise, the aft-fan must provide majority of the thrust in order to achieve minimum $TSFC$.

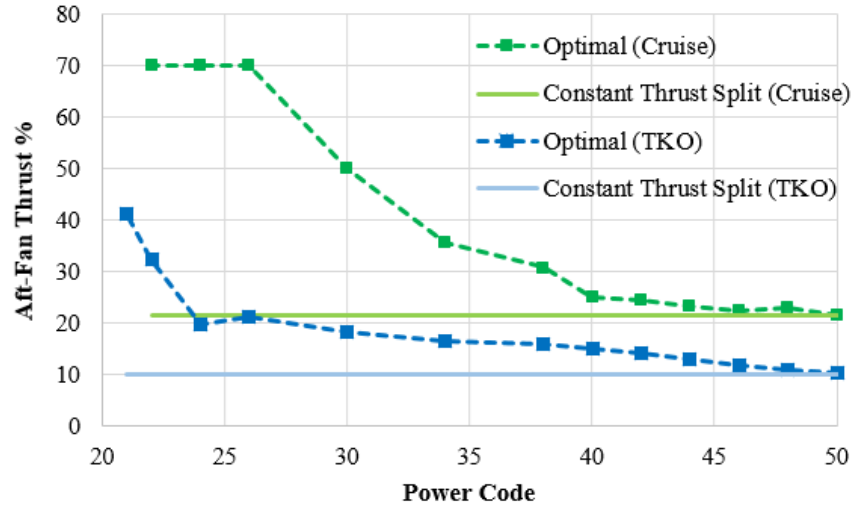


Fig. 10. BLI Aft-Fan Propulsor % Thrust

D. System Level Impacts

Finally, the system level impact of the partial-turboelectric propulsion architecture being studied were determined by using the vehicle sizing and mission analysis tools previously described (see Fig. 5). The performance of both the optimal power schedule and the constant thrust split were compared against a baseline vehicle. This baseline consists of a notional 150-pax vehicle with an engine cycle and technology assumptions that are consistent to the Far Term time frame. The additional drag produced by the BLI aft-fan (as a result of increased wetted area) were accounted for by increasing the equivalent dimensions of the underwing engines in the mission analysis code. These results, presented in Table 5, refer to a 900 nmi economic mission.

Table 5. System-level Performance Comparison

Variable	Baseline	% Difference Optimal Power	% Difference Thrust Split
<i>Block Fuel (lb)</i>	7352.46	-7.290	-4.073
<i>TOGW (lb)</i>	132518.1	+3.323	+3.809
<i>TSFC (35 kft)</i>	0.5506	-6.435	-3.109
<i>TSFC (43 kft)</i>	0.5539	-9.820	-10.107

In this exercise, it is seen that the optimizer produces little above 3% additional fuel burn reductions for this type of propulsion architecture and vehicle. These reductions are obtained regardless of the increases in *TOGW*, which are due to the additional electric components and the detailed cable weight estimation model used. Note that the *TSFC* numbers in the baseline are different than those shown in Table 4 as these were taken from the actual mission analysis outputs. It was also noted that there seem to be increased benefits for this concept if it is allowed to cruise at higher altitudes than what was used during the MDP procedure. This was examined further by plotting the resulting motor powers vs. throttle setting and *TSFC* reductions at different cruise altitudes.

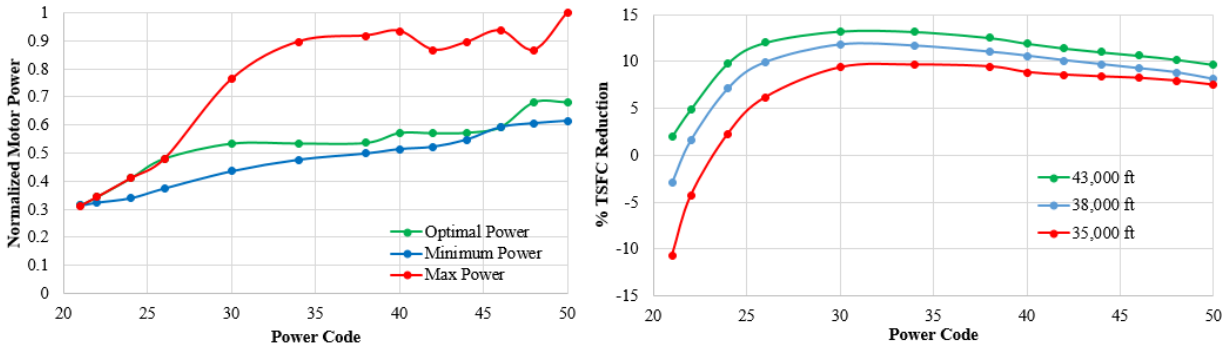


Fig. 11. Propulsion System Performance at Different Altitudes

From Figure 11, it is seen how at higher altitudes the optimal motor power lies closer to the minimum allowable power for $PC > 35$, which covers the more likely throttle settings for operation at this conditions. The figure on the right shows the $\%TSFC$ reductions and how they increase with higher altitudes. Looking at the mission summary files, it was possible to compare the performance of this partial-turboelectric propulsion architecture with respect to the baseline aircraft.

Table 6. Mission Segment Fuel Consumption Comparison

Mission Segment	% of Total Block Fuel			% Relative to Baseline	
	Baseline	Optimize	Thrust Split	Optimize	Thrust Split
Climb	23.19	23.39	22.73	+3.93	+4.05
Cruise	49.46	44.31	42.91	-7.82	-8.33
Descent	11.09	17.30	19.60	-2.78	+12.95

In Table 6, the columns under "*% of Total Block Fuel*" contain the percentage fuel consumed during each one of the main mission segments with respect to their total economic mission block fuel. To the right, the two columns under "*% Relative to Baseline*" compare the fuel consumed at each segment per minute with respect to the baseline aircraft. This analysis shows how this architecture performs better mostly during cruise, which is the largest portion of the mission and thus represents the largest fuel savings. These benefits offset the increase in fuel consumption during other segments, where the system is operating at part power (it is throttled down), and the performance of the system is worse than the baseline (see Fig. 9).

Lastly, it was desired to obtain an idea of how these system level benefits would change given some uncertainty around the estimation of the BLI benefits in the current framework. This was done by adding a multiplier factor to both P_{Kinlet} and $\Delta\Phi_{wake}$ in Eq. 5 and then running the entire model to obtain the mission fuel burn benefits. These results are shown in Fig. 12.

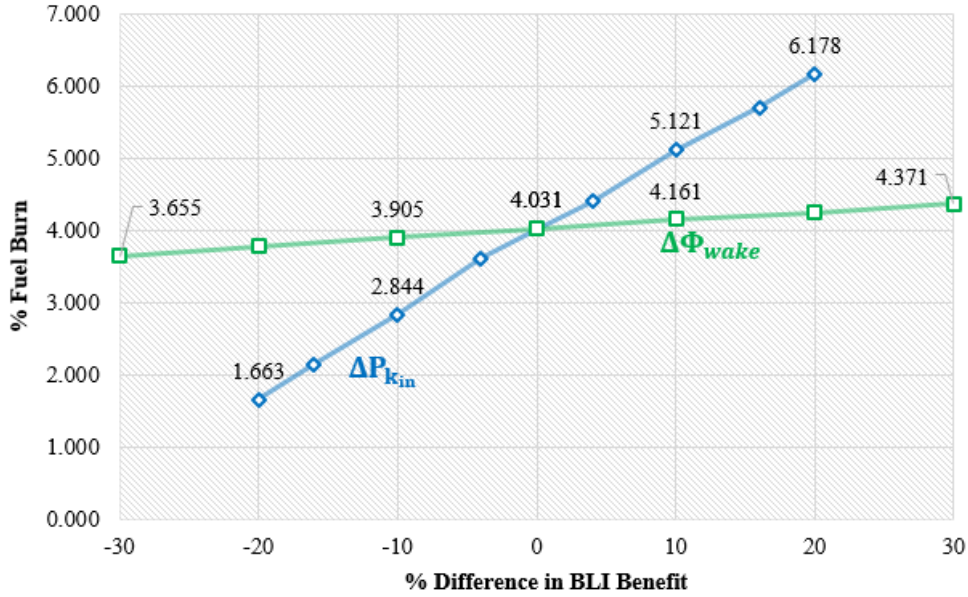


Fig. 12. Sensitivity of Fuel Burn to BLI Effects

The analysis showed that, in this partially-turboelectric propulsion architecture and with the way the BLI benefits have been quantified in this framework, BLI has a linear impact on fuel burn. The dominant effect is the $P_{K_{inlet}}$ term, which captures the effects of the reduced momentum deficit at the inlet and any pressure expansion terms. The reduction in wake dissipation has a similar impact on performance but with lesser variability.

E. Discussion

This work has shown some results that were noteworthy and deserve some further discussion in regards to the behavior of the motor power space, the effects of boundary layer ingestion, and the results from the system-level study. The use of the power balance method to quantify the BLI benefits has been gaining strength in the academic literature. There is, however, the need to convert the calculated power terms into conventional "*thrust-drag*" terms so that they can be used in conventional analysis codes such as NPSS or FLOPS. There are also opportunities to keep improving the fidelity of these BLI effects by performing CFD simulations that include a full 3-D aircraft model and can simulate a larger array of flight conditions. However this was not necessarily the focus of this paper. Instead, the goal was to explore different power management alternatives for partially-turboelectric propulsion systems.

The results shown throughout the paper show that the BLI benefits are indeed larger at cruising condition. Not surprisingly, the optimizer tends towards the max allowable power (see Fig. 8), which is expected as this is the design motor power for which the system was sized to. It is also noted that there is virtually no fuel burn benefits to be gained by using different power management schemes at low altitude-low Mach operating condition, whereas the optimizer does provide some additional benefits for a good range of throttle settings (see Fig. 9). It is important, however, to make a note that these benefits are also tied to the concept and mission under evaluation. A change in the payload and range might change the thrust requirements throughout the mission, thus changing the throttle setting and changing the expected *TSFC* reduction. In addition, the off-design performance of the electric components (see Table 1) was not modeled. The inclusion of these calculations could potentially open up the design and motor power space, would increase the variables to be considered in the optimization framework, and produce significant changes to the final benefits observed here.

Last but not least, running the optimizer was significantly more computational expensive than using the *thrust split* schedule. The results in Table 6 show that the optimizer is able to minimize fuel consumption at lower altitudes (segment "*Climb*" in the table) and during descent (low throttle). Taking into consideration that the motor power schedule was shown not to be clearly defined (such that it could be standardized for other missions), this leads to the conclusion that it would be advantageous to instead use a power management schedule that is computationally efficient (such as max power) and only use the optimizer during the descent portion of the mission.

IV. Conclusion

The goal of this work was to determine optimal and alternative power management schemes for a partially distributed turbo-electric aircraft with a boundary layer ingesting propulsor and observe its effects on propulsor and vehicle performance. This required the creation of new vehicle and engine architecture modules to be implemented in ASDL's state of the art vehicle modeling environment. The framework was heavily modified to handle new variables and parameters unique to the turbo-electric architecture. Not only was an NPSS propulsion model created and added to the environment, but a whole suite of NPSS class files were integrated as well. Additional WATE++ classes were created to calculate the weight penalty from the electrical and thermal management system required by the turbo-electric architecture. Additional class files were also created to capture the BLI effects for the propulsor using the power balance method by incorporating data from 2-D CFD in the NPSS model by using surrogate models. Lastly, additional data links were created from NPSS to CMPGEN to create a performance map for the aft-fan propulsor.

A multi-design point cycle analysis model was used to size and analyze the propulsion model, which was then used to generate engine decks to be used in the aircraft's sizing and mission analysis routines. The optimal motor power operational space was found by finding the bounds of min and max power allowable given the constraints imposed by the max motor rated power, the turbofan idle operating limits, the aft-fan max speeds, and the low-pressure compressor stall margin. A 1-D Golden Ratio line search algorithm was then implemented to find the motor power that minimized *TSFC* within those bounds.

Three alternative power management schedules were developed to compare against the optimization algorithm. The first two operated the motor at its maximum and minimum operating limits as determined by the optimization algorithm. A fourth and last schedule consisted of a constant thrust split between the turbofan engines and the aft-fan propulsor. These schedules were used to produce engine decks, which were then used to size the vehicle and perform mission analysis. This allowed to determine the system level benefits of this partial-turboelectric architecture with BLI. The results demonstrated that the motor power design space was not unique and rather differed for each flight condition, with a set of non-linear changes for different throttle settings. The results did show that the operation of the BLI fan was more beneficial at cruise and even more at higher altitudes, with the optimizer tending towards the maximum allowable power. Whereas this system showed a reduction of 4% in economic mission block fuel burn with respect to an equivalent vehicle baseline, the use of the optimizer was also shown to provide an additional 3% benefit. This opens up the possibility to implement different types of optimization strategies and power management schedules in the future that might provide even more benefits to this type of novel propulsion architectures.

Acknowledgments

The authors would like to acknowledge the support for this work provided by NASA Glenn Research Center through the Advanced Air Transport Technology (AATT) project. In addition, the valuable advice provided by ASDL's engineers Dr. Chung Lee and Jai Ahuja in quantifying the BLI benefits using CFD, and Dr. Jimmy Tai for his help in setting up the MDP partially-turboelectric model in the EDS environment.

References

- [1] Bradley, M., and Dronney, C., "Subsonic Ultra Green Aircraft Research Phase II: N+4 Advanced Concept Development," Tech. rep., NASA, 2012.
- [2] Welstead, J., and Felder, J., "Conceptual Design of a Single-Aisle Turboelectric Commercial Transport with Fuselage Boundary Layer Ingestion," *54th AIAA Aerospace Sciences Meeting*, AIAA, San Diego, CA, 2016, pp. 1–17. doi:10.2514/6.2016-1027.
- [3] Welstead, J., and Felder, J., "Overview of the NASA STARC-ABL (Rev. B) Advanced Concept,," Tech. rep., NASA, 2018.
- [4] Hall, D., Dowdle, A., Gonzales, J., Trollinger, L., and Thalheimer, W., "Assessment of a Boundary Layer Ingesting Turboelectric Aircraft Configuration using Signomial Programming," *2018 Aviation Technology, Integration, and Operations Conference*, AIAA, Atlanta, GA, 2018, pp. 1–16. doi:10.2514/6.2018-3973.
- [5] Kenway, G., and Kiris, C., "Aerodynamic Shape Optimization of the STARC-ABL Concept for Minimal Inlet Distortion," *2018 AIAA/ASCE/AHS/ASC Structures, Structural Dynamics, and Materials Conference*, AIAA, Kissimmee, Florida, 2018, pp. 1–14. doi:10.2514/6.2018-1912.
- [6] Gray, J., and Martins, J., "Coupled Aeropropulsive Design Optimisation of a Boundary-layer Ingestion Propulsor," *The Aeronautical Journal*, Vol. 123, No. 1259, 2018, pp. 1–17. doi:10.1017/aer.2018.120.

- [7] Blumenthal, B., Elmiligui, R., Geiselhart, K., Campbell, R., Maughmer, M., and Schmitz, S., “Computational Investigation of a Boundary-Layer Ingesting Propulsion System for the Common Research Model,” *46th AIAA Fluid Dynamics Conference*, AIAA, Washington, DC, 2016, pp. 1–32. doi:10.2514/6.2016-3812.
- [8] Gladin, J., “A Sizing and Vehicle Matching Methodology for Boundary Layer Ingesting Propulsion Systems,” Ph.D. thesis, Georgia Institute of Technology, 2015.
- [9] Hall, D., Huang, A., Uranga, A., Greitzer, E., Drela, M., , and Sato, S., “Boundary Layer Ingestion Propulsion Benefit for Transport Aircraft,” *Journal of Propulsion and Power*, Vol. 33, No. 5, 2017, pp. 1118–1129. doi:10.2514/1.B36321.
- [10] Smith, L., “Wake Ingestion Propulsion Benefit,” *Journal of Propulsion and Power*, Vol. 9, No. 1, 1993, pp. 74–82. doi: 10.2514/3.11487.
- [11] Hendricks, E., “A Review of Boundary Layer Ingestion Modeling Approaches for use in Conceptual Design,” Tech. rep., NASA, 2018.
- [12] Gladin, J., Trawick, D., Perullo, C., Tai, J., and Mavris, D., “Modeling and Design of a Partially Electric Distributed Aircraft Propulsion System with GT-HEAT,” *AIAA SciTech 2017 Forum*, AIAA, Grapevine, Texas, 2017, pp. 1–18. doi: 10.2514/6.2017-1924.
- [13] Perullo, C., Trawick, D., Clifton, W., Tai, J., and Mavris, D., “Development of a Suite of Hybrid Electric Propulsion Modeling Elements Using NPSS,” *ASME Turbo Expo 2014*, Asme, Düsseldorf, Germany, 2014, pp. 1–15. doi:10.1115/GT2014-27047.
- [14] Kowalski, E., “A Computer Code for Estimating Installed Performance of Aircraft Gas Turbine Engines,” Tech. rep., NASA, 1979.
- [15] Torenbeek, E., *Synthesis of Subsonic Airplane Design*, Springer, Dordrecht, Netherlands, 1982.
- [16] Gray, J., Mader, C., Kenway, G., and Martins, J., “Modeling Boundary Layer Ingestion Using a Coupled Aeropropulsive Analysis,” *Journal of Aircraft*, Vol. 55, No. 3, 2018, pp. 1191–1199. doi:10.2514/1.C034601.
- [17] Hall, D., Lieu, M., and Drela, M., “Aerodynamic Performance Accounting for Ultra-Integrated Air Vehicle Configurations,” *AIAA SciTech 2019 Forum*, AIAA, San Diego, California, 2019, pp. 1–15. doi:10.2514/6.2019-1310.
- [18] Pokhrel, M., Shi, M., Ahuja, J., Gladin, J., and Mavris, D., “Conceptual Design of a BLI Propulsor Capturing Aero-Propulsive Coupling and Distortion Impacts,” *AIAA SciTech 2019 Forum*, AIAA, San Diego, California, 2019, pp. 1–13. doi:10.2514/6.2019-1588.
- [19] Kirby, M., and Mavris, D., “The Environmental Design Space,” *26th International Congress of the Aeronautical Sciences*, ICAS, Anchorage, Alaska, 2008, pp. 1–9.
- [20] Barros, P., Kirby, M., and Mavris, D., “An Approach for Verification and Validation of the Environmental Design Space,” *26th International Congress of the Aeronautical Sciences*, AIAA, Anchorage, Alaska, 2008, pp. 1–15. doi:10.2514/6.2008-8875.
- [21] Schutte, J., “Simultaneous Multi-design Point Approach to Gas Turbine On-design Cycle Analysis for Aircraft Engines,” Ph.D. thesis, Georgia Institute of Technology, 2009.
- [22] Campbell, A., “Architecting Aircraft Power Distribution Systems Via Redundancy Allocation,” Ph.D. thesis, Georgia Institute of Technology, 2014.
- [23] Vanderplaats, G., *Multidiscipline Design Optimization*, Vanderplaats Research and Development Inc., Monterey, California, 2007.
- [24] Converse, G., and Giffin, R., “Extended Parametric Representation of Compressors Fans and Turbines. Vol. I - CMGEN User’s Manual,” Tech. rep., NASA, 1984.